Research Article ISSN 2832-9384

Journal of Materials and Polymer Science

Plane Strain State of Composite Material Reinforced by Two Rows of Crystalline Fibres in Dynamic Elastic-Plastic Formulation

Vladislav Bogdanov

Progressive Research Solutions Pty. Ltd.

***Correspondence author**
Vladislav Bogdanov,
Progressive Research Solutions Pty. Ltd.
28/2 Buller Rd, Artarmon, Sydney,
Australia 2064.

Submitted : 7 June 2023 ; Published : 11 July 2023

Citation : Bogdanov, V (2023). Plane Strain State of Composite Material Reinforced by Two Rows of Crystalline Fibres in Dynamic Elastic-Plastic Formulation. *J mate poly sci, 3*(3): 1-6. DOI : https://doi.org/10.47485/2832-9384.1034

Abstract
A generalized approach was developed for solving contact problems in a dynamic elastic-plastic formulation. For the design of composite and reinforced materials, a technique for solving dynamic contact problems in more adequate an elastic-plastic mathematical formulation is used. To consider the physical nonlinearity of the deformation process, the method of successive approximations is used, which makes it possible to reduce the nonlinear problem to a solution of the sequences of linear problems. In contrast to the traditional plane strain, when one normal stress is equal to a certain constant value, for a more accurate description of the deformation of the sample, taking into account the possible increase in longitudinal elongation, we present this normal stress as a function that depends on the parameters that describe the bending of a prismatic body that is in a plain strain state. The problem of a plane strain state of a beam made from the composite reinforced one-layer material is being solved. The reinforced or armed composite material consists of two materials: the main material of glass and two rows of the reinforcing crystalline fourteen fibres of basalt. Glass has high strength and is not affected by the processes of aging of the material, corrosion, and creep. In addition, this material is cheap and widely available. The reinforced composite beam is rigidly linked to an absolutely solid base and on which an absolutely solid impactor acts from above in the centre on a different size of the area of initial contact.

Keywords: Plane, strain, stress, state, impact, composite, armed, reinforced, material, elastic-plastic, deformation.

Introduction

The use of a generalized approach to solving dynamic contact problems in an elastic-plastic formulation makes it possible to use it to solve contact problems for a body of arbitrary shape, which is subjected to an arbitrary distributed over the contact zone or shock loading.

Since glass is a cheap, ubiquitous material that is not susceptible to corrosion and aging and creep processes, like metals and alloys, the study of composite materials containing glass is relevant and actual. Glass is also convenient in that it can be poured into the frame of the reinforcement and thus can be further strengthened. As reinforcing elements, metal wire, polysilicate, polymer, polycarbon, crystalline compounds, which can have a fairly small thickness, can be used.

In (Bogdanov, 2023; Bogdanov, 2022; Bogdanov, 2022; Bogdanov, 2022; Bogdanov, 2022), a new approach to solving the problems of impact and nonstationary interaction in the elastoplastic mathematical formulation was developed. In these papers like in non-stationary problems (Bogdanov, 2023; Bogdanov, 2022; Bogdanov, 2022; Bogdanov, 2022; Bogdanov, 2022), the action of the striker is replaced by a distributed load in the contact area, which changes according to a linear law. The contact area remains constant.

The solution of problems for composite cylindrical shells (Lokteva et al., 2020), elastic half-space (Igumnov et al., 2013), elastic layer (Kuznetsova et al., 2013), elastic rod (Fedotenkov et al., 2019; Vahterova & Fedotenkov, 2020) were developed using method of the influence functions (Gorshkov & Tarlakovsky, 1985).

In (Bogdanov, 2022; Bogdanov, 2022; Bogdanov, 2022; Bogdanov, 2022) dynamic interaction process of plane hard body and two layers reinforced composite material was investigated and the fields of summary plastic deformations and normal stresses arising in the base are calculated using plane strain (Bogdanov, 2022; Bogdanov, 2022; Bogdanov, 2022; Bogdanov, 2022) and plane stress (Bogdanov, 2022) states models. In (Bogdanov, 2022) results are depending on the size of the area of an initial contact between the impactor and the upper surface of the base. In (Bogdanov, 2022) results were calculated depending on the thickness of top metal layer of the composite base. In (Bogdanov, 2022) results were calculated depending on the material of top layer of the composite base. It was investigated composite bases reinforced by steel, titanium and aluminium top layers.

In contrast from the work (Bogdanov, 2018), in this paper, we investigate the impact process of hard body with plane area of its surface on the top of the composite beam which consists main glass layer reinforced by seven crystalline basalt fibers.

Problem Formulation

Deformations and their increments (Bogdanov, 2023), Odquist parameter $\kappa = \int d\varepsilon_i^p$ (ε_i^p is plastic deformations intensity), stresses are obtained from the numerical solution of the dynamic elastic-plastic interaction problem of infinite composite beam $\{-L/2 \le x \le L/2; 0 \le y \le B; -\infty \le z \le \infty\}$, in the plane of its cross section in the form of rectangle. It is assumed that the stress-strain state in each cross section of the beam is the same, close to the plane deformation, and therefore it is necessary to solve the equation for only one section in the form of a rectangle Σ = L x B with two materials: main glass layer $\{-L/2 \le x \le L/2; -\infty \le z \le \infty; 0 \le y \le B\}$ and two rows of fourteen reinforcing crystalline basalt fibres $\{|x| \le b_1; -\infty \le z \le \infty; h_2 - h \le y \le h_2\}$, $\{b_i \le |x| \le b_{i+1}; -\infty \le z \le \infty; h2 - h \le y \le h2\}$, $\{|x| \le b1; -\infty \le z \le \infty; B - h1 - h \le y \le h1\}$, $\{bi \le |x| \le bi+1; B - h1 - h \le B - h1\}$ $(i=2; 4; 6)$. The contact between glass and basalt fibres is ideally rigid. We assume that the contact between the lower surface of the reinforced glass base and the absolute hard half-space $\{y \le 0\}$ is ideally rigid.

From above on a body the absolutely rigid drummer contacting along a segment $\{|x| \le A; y = B\}$. Its action is replaced by an even distributed stress $-P$ in the contact region, which changes over time as a linear function $P = p_{01} + p_{02}t$. Given the symmetry of the deformation process relative to the line x=0, only the right part of the cross section is considered below (Fig. 1). The calculations use known methods for studying the quasi-static elastic-plastic (Bogdanov, 2023; Mahnenko, 1976; Mahnenko, 2003; Mahnenko et al., 2009) model, considering the non-stationarity of the load and using numerical integration implemented in the calculation of the dynamic elastic model (Bogdanov, 2023; Bogdanov, 2022; Bogdanov, 2022; Bogdanov, 2022; Bogdanov, 2022).

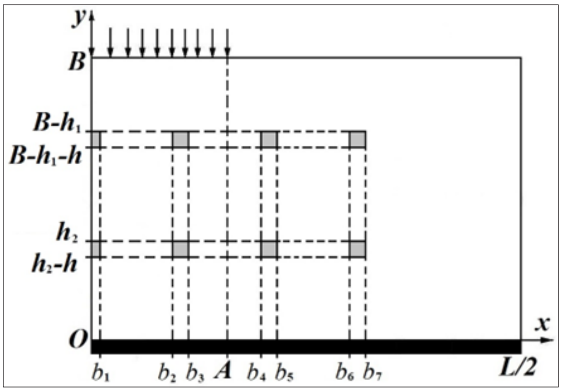

Fig. 1: Geometric scheme of the problem

The equations of the plane dynamic theory are considered, for which the components of the dis-placement vector $\mathbf{u} = (u_x, u_y)$ are related to the components of the strain tensor by Cauchy relations:

$$\varepsilon_{xx} = \frac{\partial u_x}{\partial x}, \ \varepsilon_{yy} = \frac{\partial u_y}{\partial y}, \ \varepsilon_{xy} = \frac{1}{2}\left(\frac{\partial u_x}{\partial y} + \frac{\partial u_y}{\partial x}\right).$$

The equations of motion of the medium have the form:

$$\frac{\partial \sigma_{xx}}{\partial x} + \frac{\partial \sigma_{xy}}{\partial y} = \rho \frac{\partial^2 u_x}{\partial t^2}, \ \ \frac{\partial \sigma_{xy}}{\partial x} + \frac{\partial \sigma_{yy}}{\partial y} = \rho \frac{\partial^2 u_y}{\partial t^2}, \qquad (1)$$

where p– material density.

The boundary and initial conditions of the problem have the form:

$$\begin{aligned} &x = 0, \ 0 < y < B: \ u_x = 0, \ \sigma_{xy} = 0, \\ &x = L/2, \ 0 < y < B: \ \sigma_{xx} = 0, \ \sigma_{xy} = 0, \\ &y = 0, \ 0 < x < L/2: \ u_y = 0, \ \sigma_{xy} = 0, \\ &y = B, \ 0 < x < A: \ \sigma_{yy} = -P, \ \sigma_{xy} = 0, \\ &y = B, \ A < x < L/2: \ \sigma_{yy} = 0, \ \sigma_{xy} = 0. \end{aligned} \qquad (2)$$

$$u_x\big|_{t=0} = 0, \ u_y\big|_{t=0} = 0, \ u_z\big|_{t=0} = 0, \ \dot{u}_x\big|_{t=0} = 0, \ \dot{u}_y\big|_{t=0} = 0, \ \dot{u}_z\big|_{t=0} = 0. \qquad (3)$$

The determinant relations of the mechanical model are based on the theory of non-isothermal plastic flow of the medium with hardening under the condition of Huber-Mises fluidity. The effects of creep and thermal expansion are neglected. Then, considering the components of the strain tensor by the sum of its elastic and plastic components (Kachanov, 1969; Collection: Theory of plasticity IL, 1948), we obtain expression for them:

$$\varepsilon_{ij} = \varepsilon_{ij}^e + \varepsilon_{ij}^p, \ d\varepsilon_{ij}^p = s_{ij} d\lambda, \ \varepsilon_{ij}^e = \frac{1}{2G} s_{ij} + K\sigma + \varphi. \qquad (4)$$

here $s_{ij} = \sigma_{ij} - \delta_{ij}\sigma$ – stress tensor deviator; δ_{ij} – Kronecker symbol; E – modulus of elasticity (Young's modulus); G – shear modulus; $K_1 = (1 - 2v)/(3E)$, $K = 3K_1$–volumetric compression modulus, which binds in the ratio $\varepsilon = K\sigma + \phi$ volumetric expansion 3ε (thermal expansion $\phi = 0$); $\sigma = (\sigma_{xx} + \sigma_{yy} + \sigma_{zz})/3$ – mean stress; $d\lambda$ –some scalar function (Mahnenko, 1976), which is determined by the shape of the load surface and we assume that this scalar function is quadratic function of the stress deviator s_{ij} (Mahnenko, 1976; Kachanov, 1969; Collection: Theory of plasticity IL, 1948).

$$d\lambda = \begin{cases} 0 \quad (f \equiv \sigma_i^2 - \sigma_S^2(T) < 0) \\ \dfrac{3d\varepsilon_i^p}{2\sigma_i} \quad (f = 0, df = 0) \\ (f > 0 - \text{inadmissible}) \end{cases}, \qquad (5)$$

$$d\varepsilon_i^p = \frac{\sqrt{2}}{3}\left(\left(d\varepsilon_{xx}^p - d\varepsilon_{yy}^p\right)^2 + \left(d\varepsilon_{xx}^p - d\varepsilon_{zz}^p\right)^2 + \left(d\varepsilon_{yy}^p - d\varepsilon_{zz}^p\right)^2 + 6\left(d\varepsilon_{xy}^p\right)^2\right)^{1/2},$$

$$\sigma_i = \frac{1}{\sqrt{2}}\left(\left(\sigma_{xx} - \sigma_{yy}\right)^2 + \left(\sigma_{xx} - \sigma_{zz}\right)^2 + \left(\sigma_{yy} - \sigma_{zz}\right)^2 + 6\sigma_{xy}^2\right)^{1/2}.$$

It should be noted that the developed algorithm makes it possible to use the function f in (5) not only in the form of a quadratic function (in this case, we obtain the plastic fluidity condition in the Huber-Mises form), however also in the form of a function containing terms of third and higher degrees. This statement requires further research.

The material is strengthened with a hardening factor η^* (Bogdanov, 2023; Bogdanov, 2022; Bogdanov, 2022; Bogdanov, 2022; Bogdanov, 2022; Mahnenko, 1976):

$$\sigma_S(T) = \sigma_{02}(T_0)\left(1+\frac{\kappa(T)}{\varepsilon_0}\right)^{\eta^*}, \quad \varepsilon_0 = \frac{\sigma_{02}(T_0)}{E}, \tag{6}$$

where T – temperature; K – Odquist parameter, $T_0 = 20^{\circ}$C, η^* – hardening coefficient; $\sigma_S(T)$ – yield strength after hardening of the material at temperature T. Rewrite (4) in expanded form:

$$d\varepsilon_{xx} = d\left(\frac{\sigma_{xx}-\sigma}{2G}+K\sigma\right)+(\sigma_{xx}-\sigma)d\lambda, \quad d\varepsilon_{yy} = d\left(\frac{\sigma_{yy}-\sigma}{2G}+K\sigma\right)+(\sigma_{yy}-\sigma)d\lambda,$$
$$d\varepsilon_{zz} = d\left(\frac{\sigma_{zz}-\sigma}{2G}+K\sigma\right)+(\sigma_{zz}-\sigma)d\lambda, \quad d\varepsilon_{xy} = d\left(\frac{\sigma_{xy}}{2G}\right)+\sigma_{xy}d\lambda, \tag{7}$$

In contrast to the traditional plane deformation, when $\Delta\mathcal{E}_{zz}$ (x, y)= constant, for a refined description of the deformation of the specimen, taking into account the possible increase in longitudinal elongation $\Delta\mathcal{E}_{zz}$, we present in its form (Bogdanov, 2023; Boli & Waner, 1964):

$$\Delta\varepsilon_{zz}(x,y) = \Delta\varepsilon_{zz}^0 + \Delta\chi_x x + \Delta\chi_y y, \tag{8}$$

where unknown $\Delta\gamma_x$ and $\Delta\gamma_y$ describe the bending of the prismatic body (which simulates the plane strain state in the solid mechanics) in the Ozx and Ozy planes, respectively, and $\Delta\varepsilon_{zz}^0$ – the increments according to the detected deformation bending along the fibres $x = y = 0$.

Solution Algorithm

Let the nonstationary interaction (Bogdanov, 2023) occur in a time interval $t \in [0, t_*]$. Then for every moment of time t:

$$\varepsilon_{xx}^e = \frac{\sigma_{xx}-\sigma}{2G}+K\sigma, \quad \varepsilon_{yy}^e = \frac{\sigma_{yy}-\sigma}{2G}+K\sigma, \quad \varepsilon_{zz}^e = \frac{\sigma_{zz}-\sigma}{2G}+K\sigma, \quad \varepsilon_{xy}^e = \frac{\sigma_{xy}}{2G}, \tag{9}$$

$$\frac{d\varepsilon_{xx}^p}{dt} = \left(\sigma_{xx}-\sigma\right)\frac{d\lambda}{dt}, \quad \frac{d\varepsilon_{xy}^p}{dt} = \sigma_{xy}\frac{d\lambda}{dt}, \quad \frac{d\varepsilon_{yy}^p}{dt} = \left(\sigma_{yy}-\sigma\right)\frac{d\lambda}{dt}, \quad \frac{d\varepsilon_{zz}^p}{dt} = \left(\sigma_{zz}-\sigma\right)\frac{d\lambda}{dt}.$$

For numerical integration over time, Gregory's quadrature formula (Bogdanov, 2023; Hemming, 1972) of order m_1 = 3 with coefficients D_n was used. After discretisation in time with nodes $t_k = k\Delta t \in [0, t_*]$ $(k = 0, K)$ for each value k we write down the corresponding node values of deformation increments:

$$\Delta\varepsilon_{xx,k} = B_1\sigma_{xx,k} + B_2\sigma_{yy,k} - \beta_{xx}, \quad \Delta\varepsilon_{yy,k} = B_2\sigma_{xx,k} + B_1\sigma_{yy,k} - \beta_{yy},$$
$$\Delta\varepsilon_{zz,k} = \alpha_1\sigma_{zz,k} + \alpha_2(\sigma_{xx,k} - \sigma_{yy,k}) - b_{zz}, \quad \Delta\varepsilon_{xy,k} = B_3\sigma_{xy,k} - b_{xy},$$
$$\beta_{xx} = b_{xx} - \alpha_2(b_{zz} + \Delta\varepsilon_{zz})/\alpha_1, \; \beta_{yy} = b_{yy} - \alpha_2(b_{zz} + \Delta\varepsilon_{zz})/\alpha_1, \; \beta_{zz} = -(b_{zz} + \Delta\varepsilon_{zz})/\alpha_1,$$
$$B_1 = \frac{\alpha_1^2 - \alpha_2^2}{\alpha_1}, \quad B_2 = \frac{\alpha_2(\alpha_1 - \alpha_2)}{\alpha_1}, \quad B_3 = \frac{1}{2G} + D_0\Delta\lambda_k,$$
$$\alpha_1 = \frac{1}{3}\left(K + \frac{1}{G} + 2D_0\Delta\lambda_k\right), \quad \alpha_2 = \frac{1}{3}\left(K - \frac{1}{2G} - D_0\Delta\lambda_k\right),$$
$$b_{ij} = \frac{1}{2G}\sigma_{ij,k-1} + \delta_{ij}\left(K - \frac{1}{2G}\right)\sigma_{k-1} - \sum_{n=1}^{m_1} D_n\left(\sigma_{ij,k-n} - \delta_{ij}\sigma_{k-n}\right)\Delta\lambda_{k-n} \quad (i,j = x,y,z). \tag{10}$$

The solution of the system (10), gives expressions for the components of the stress tensor at each step [1]:

$$\sigma_{xx,k} = A_1\Delta\varepsilon_{xx,k} + A_2\Delta\varepsilon_{yy,k} + Y_{xx}, \quad \sigma_{yy,k} = A_2\Delta\varepsilon_{xx,k} + A_1\Delta\varepsilon_{yy,k} + Y_{yy},$$
$$\sigma_{zz,k} = -\alpha_2(\sigma_{xx,k} + \sigma_{yy,k})/\alpha_1 - \beta_{zz}, \quad \sigma_{xy,k} = A_3\Delta\varepsilon_{xy,k} + Y_{xy},$$
$$Y_{xx} = A_1\beta_{xx} + A_2\beta_{yy}, \quad Y_{yy} = A_2\beta_{xx} + A_1\beta_{yy}, \quad Y_{xy} = A_3 b_{xy}, \quad A_3 = 1/B_3,$$
$$A_1 = B_1\Big/\left(B_1^2 - B_2^2\right), \quad A_2 = -B_2\Big/\left(B_1^2 - B_2^2\right). \tag{11}$$

Function $\psi = 1/(2G) + \Delta\lambda$, which is characterizing the yield condition, taking into account (8), (9) and (11) is:

$$\psi = \begin{cases} \dfrac{1}{2G} \quad (f < 0) \\ \dfrac{1}{2G} + \dfrac{3\Delta\varepsilon_i^p}{2\sigma_i} \quad (f = 0, df = 0), \\ (f > 0 - \text{inadmissible}) \end{cases} \tag{12}$$

$$\Delta\varepsilon_i^p = \frac{\sqrt{2}}{3}\left(\left(\Delta\varepsilon_{xx}^p - \Delta\varepsilon_{yy}^p\right)^2 + \left(\Delta\varepsilon_{xx}^p - \Delta\varepsilon_{zz}^p\right)^2 + \left(\Delta\varepsilon_{yy}^p - \Delta\varepsilon_{zz}^p\right)^2 + 6\left(\Delta\varepsilon_{xy}^p\right)^2\right)^{1/2},$$
$$\Delta\varepsilon_{xx}^p = \Delta\varepsilon_{xx} - \Delta\varepsilon_{xx}^e, \quad \Delta\varepsilon_{yy}^p = \Delta\varepsilon_{yy} - \Delta\varepsilon_{yy}^e, \quad \Delta\varepsilon_{xy}^p = \Delta\varepsilon_{xy} - \Delta\varepsilon_{xy}^e, \quad \Delta\varepsilon_{zz}^p = \Delta\varepsilon_{zz} - \Delta\varepsilon_{zz}^e,$$
$$\Delta\varepsilon_{xx}^e = \frac{1}{2G}\sigma_{xx} + \left(K - \frac{1}{2G}\right)\sigma, \quad \Delta\varepsilon_{yy}^e = \frac{1}{2G}\sigma_{yy} + \left(K - \frac{1}{2G}\right)\sigma,$$
$$\Delta\varepsilon_{zz}^e = \frac{1}{2G}\sigma_{zz} + \left(K - \frac{1}{2G}\right)\sigma, \quad \Delta\varepsilon_{xy}^e = \frac{1}{2G}\sigma_{xy}, \quad \sigma = \frac{\sigma_{xx} + \sigma_{yy} + \sigma_{zz}}{3}.$$

Considering when calculating the value $\Delta\varepsilon_{zz}^p$, we found that its impact is so small that without reducing the accuracy of calculations can be considered $\Delta\varepsilon_{zz}^p = 0$.

To take into account (Bogdanov, 2023) the physical nonlinearity contained in conditions (12), the method of successive approximations is used, which makes it possible to reduce a nonlinear problem to a sequence of linear problems (Bogdanov, 2023; Mahnenko, 1976; Mahnenko, 2003; Mahnenko et al., 2009):

$$\psi^{(n+1)} = \left\{\psi^{(n)}p + \frac{1-p}{2G}, \text{ if } \sigma_{iS} < -Q; \; \psi^{(n)}, \text{ if } -Q < \sigma_{iS} < Q; \; \psi^{(n)}\frac{\sigma_i^{(n)}}{\sigma_S(T)}, \text{ if } \sigma_{iS} > Q\right\},$$
$$\sigma_{iS} = \sigma_i^{(n)} - \sigma_S(T), \tag{13}$$

where Q – the value of the largest deviation of the stress intensity $\sigma_i^{(n)}$ in step n from the strengthened yield strength; n – is the approximation number.

Unknown (Hemming & Waner, 1964) $\Delta\gamma_x$ and $\Delta\gamma_y$ (8) are determined from the conditions of equilibrium of even with respect to x normal stresses σ_{zz}.

$$\iint_{\Sigma} \sigma_{zz}(x,y)\rho\, dxdy = M_\rho, \quad (\rho = 1, x, y), \tag{14}$$

when $M_I = M_x = M_y = 0$; where M_I – projection on the axis Oz of the main vector of contact stresses, and M_x, M_y – corresponding projections of the main moment of the forces acting on the resistance (no torsion, as noted). Given the symmetry of the problem and $\sigma_{zz}(x,y) = \sigma_{zz}(-x,y)$ this equation in case of $p = x$ is satisfied automatically.

If we substitute (8) and (11) in (14), taking into account the symmetry of the integration domain with respect to x and the even of functions $\sigma_{xx,k}, \sigma_{yy,k}, b_{zz}$, we have $\Delta\gamma_x = 0$.
A system of linear al-gebraic equations is obtained for the calculation of $\Delta\varepsilon_{zz}^0$, $\Delta\chi_y$:

$$\Delta\varepsilon_{zz}^{0} L_{\rho 1} + \Delta\chi_y L_{\rho y} = \bar{M}_{\rho},\ (\rho = 1, y),$$

$$\bar{M}_{\rho} = \iint_{\Sigma} \frac{\alpha_2\left(\sigma_{xx}+\sigma_{yy}\right) - b_{zz}}{\alpha_1} \rho r dx dy,\quad L_{\rho r} = \iint_{\Sigma} \frac{\rho r dx dy}{\alpha_1},\ (r, \rho = 1, x, y). \qquad (15)$$

The stresses and strains used above were determined for each unit cell from the numerical solution at each point in time $t_k = k\Delta t$.

Numerical Solution

For both problems the explicit scheme of the finite difference method was used with a variable partitioning step along the axes Ox (M elements) and Oy (N elements). The step between the split points was the smallest in the area of the layers contact and at the boundaries of the computational domain. Since the interaction process is fleeting, this did not affect the accuracy in the first thin layer, areas near the boundaries, and the adequacy of the contact interaction modelling.

The use of finite differences (Hemming, 1972) with variable partition step for wave equations is justified in (Zukina, 2004), and the accuracy of calculations with an error of no more than $O\left((\Delta x)^2 + (\Delta y)^2 + (\Delta t)^2\right)$ where Δx, Δy and Δt – increments of variables: spatial x and y and time t. A low rate of change in the size of the steps of the partition mesh was ensured. The time step was constant.

The resolving system of linear algebraic equations with a banded symmetric matrix was solved by the Gauss method according to the Cholesky scheme.

In (Weisbrod& Rittel, 2000), during experiments, compact samples were destroyed in 21 – 23ms. The process of destruction of compact specimens from a material of size and with contact loading as in (Weisbrod & Rittel, 2000) was modelled in a dynamic elastoplastic formulation as plane strain state, considering the unloading of the ma-terial and the growth of a crack according to the local criterion of brittle fracture. The samples were destroyed in 23ms. This confirms the correctness and adequacy of the developed formulation and model.

Figures. 2 – 19 show the results of calculations of one layer specimens with a hardening factor of the material η* = 0.05. The main has made from quartz glass. The reinforcing fibres have made from bas-alt. Contact between glass and basalt is an ideal. Calculations were made at the following parameter values: temperature $T = 50^{o}$C; $L = 20mm$; $B = 5mm$; $h = 0.1mm$; $\Delta t = 3.21\text{-}10^{-8}\ s$; $p_{01} = 8\ MPa$; $p_{02} = 10\ MPa$; $M = 94$; N = 103. The smallest splitting step was 0,02mm, and the largest 0,82mm (only the first layer); $\Delta x_{\max} = 0{,}82\ mm$; $\Delta y_{\max} = 0{,}05\ mm$); $b_1 = h/2$; $b_2 = 1{,}05mm$; $b_4 = 2{,}15mm$; $b_6 = 3{,}25mm$; $b_i = b_{i-1} + h$, $(i = 3,5,7)$.

At the Figures. 2 – 10 and 11 – 19 show resalts of numerical solution of problems when the contact zone was equal $a = 2A = a_1 = 8mm$ and $a = a_2 = 3mm$, respectively.

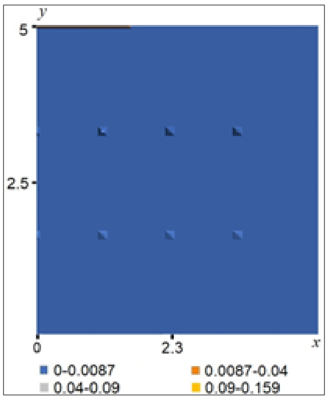

Fig. 2: Odquist parameter K when $a = a_1$ and $t = t_1$

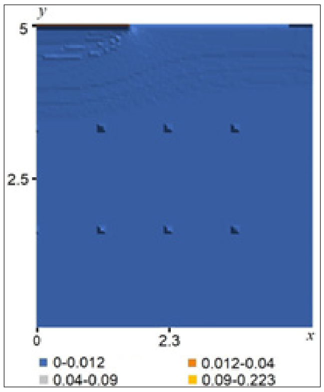

Fig. 3: Odquist parameter K when $a = a_1$ and $t = t_2$

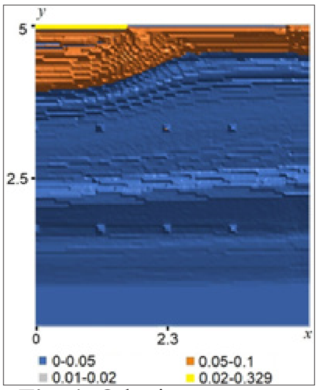

Fig. 4: Odquist parameter K when $a = a_1$ and $t = t_3$

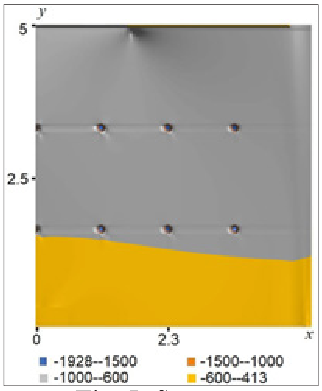

Fig. 5: Stress σ_{xx} when $a = a_1$ and $t = t_1$

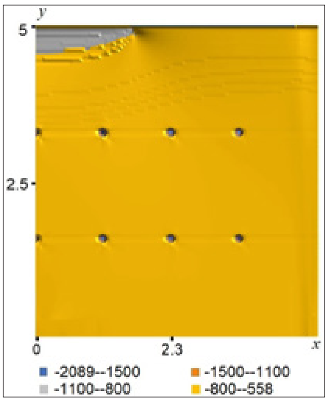

Fig. 6: Stress σ_{xx} when $a = a_1$ and $t = t_2$

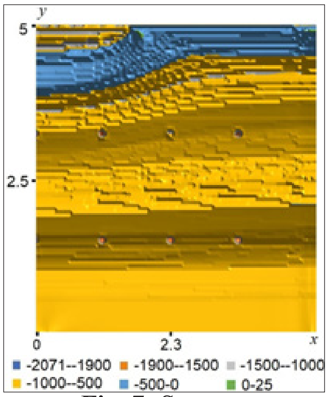

Fig. 7: Stress σ_{xx} when $a = a_1$ and $t = t_3$

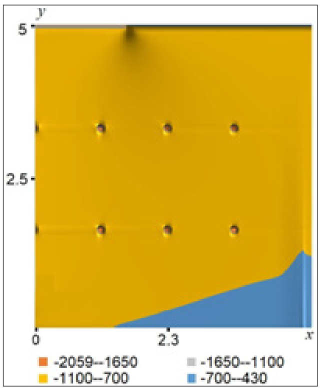

Fig. 8: Stress σ_{yy} when $a = a_1$ and $t = t_1$

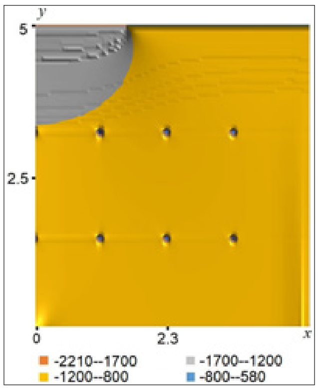

Fig. 9: Stress σ_{yy} when $a = a_1$ and $t = t_2$

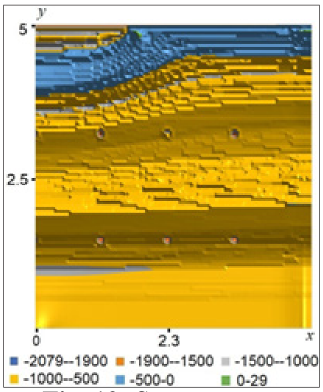

Fig. 10: Stress σ_{yy} when $a = a_1$ and $t = t_3$

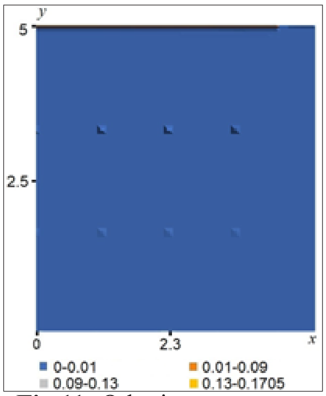

Fig.11: Odquist parameter K when $a = a_2$ and $t = t_1$

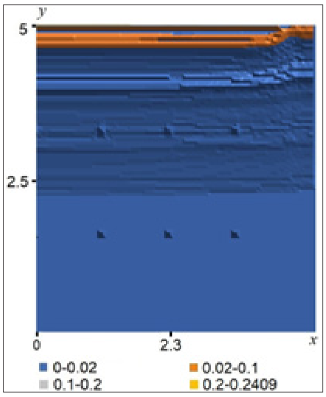

Fig. 12: Odquist parameter K when $a = a_2$ and $t = t_2$

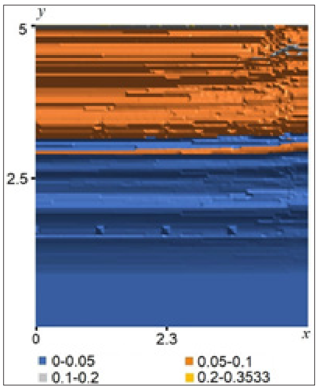

Fig. 13: Odquist parameter K when $a = a_2$ and $t = t_3$

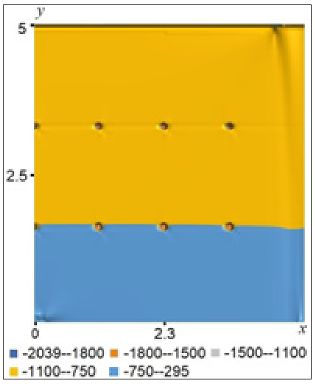

Fig. 14: Stress σ_{xx} when $a = a_2$ and $t = t_1$

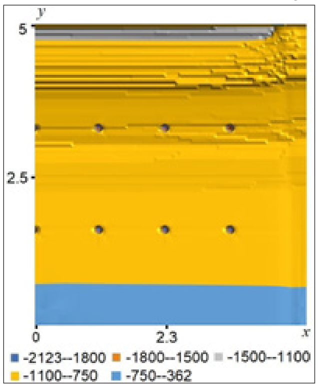

Fig. 15: Stress σ_{xx} when $a = a_2$ and $t = t_2$

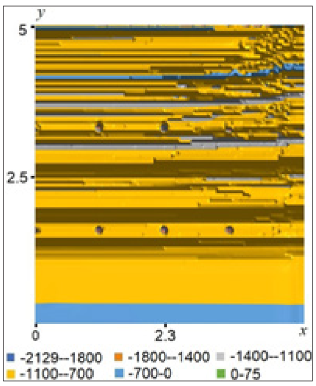

Fig. 16: Stress σ_{xx} when $a = a_2$ and $t = t_3$

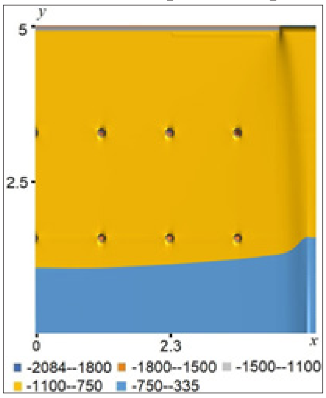

Fig. 17: Stress σ_{yy} when $a = a_2$ and $t = t_1$

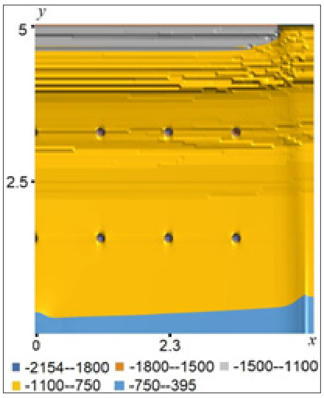

Fig.18: Stress σ_{yy} when $a = a_2$ and $t = t_2$

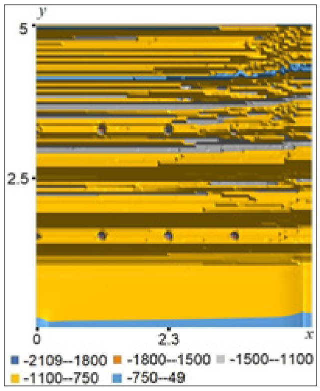

Fig. 19: Stress σ_{yy} when $a = a_2$ and $t = t_3$

Figs. 2, 5, 8, 11, 14, 17; 3, 6, 9, 12, 15, 18; 4, 7, 10, 13, 16, 19 show the fields of the Odquist parameter K, normal stresses σ_{xx} and σ_{yy} at times $t_1 = 5.46 \cdot 10^{-6}\ s$, $t_2 = 5.78 \cdot 10^{-6}\ s$ and $t_3 = 6.1 \cdot 10^{-6}\ s$ respectively.

Figs. 9 – 20 show that the highest stresses occur in the upper layer of the metal and the process of accumulation of plastic deformations is more intense there. These Figs. show areas where the normal stresses in layers are tensile. This is due to the fact that compressive stresses arise in the upper layer quickly and the contact between the layers and the contact of the lower boundary of the lower layer with an absolutely rigid base are ideally rigid.

At Fig. 2 – 4, 11 – 13 it can be seen that the greatest plastic deformations occur in a thin layer un-der the contact zone. This confirms the need to strengthen the glass layer with a thin layer of steel/metal on the upper surface of the base (Bogdanov, 2023; Bogdanov, 2022; Bogdanov, 2022; Bogdanov, 2022; Bogdanov, 2022). Fig. 5 – 10 and 14 – 19 show how stresses are concentrated in the vicinity of crystalline basalt fibres. At the moments of time t_1 and t_2, in the vicinity of basalt fibres, the absolute values of normal stresses are more than twice as high as the absolute value of stresses in other areas. Crystalline basalt fibres affect the distribution of stresses and work as concentrators of these stresses.

When the contact zone $a = a_1$, at the moment of time t_3 at a depth of about 1*mm* from the upper surface of the base, an area arises where the absolute value of normal stresses drops sharply and reaches a value of –35 *MPa*. This arises due to the fact that the process of interaction and the resulting stresses are of a wave nature. In the case of a smaller contact zone, when $a = a_2$, at the moment of time $t = t_3$, such areas appear at approximately the same depth of 1*mm* from the upper surface of the base under the contact zone, however, the normal stresses σ_{xx} and σ_{yy} there become tensile and reach values 253 *MPa* and 268 *MPa*, respectively. This most likely corresponds to the fact that the process of destruction of the material takes place in this area.

It is of interest to investigate the process of non-stationary interaction of the considered material reinforced with thicker basalt crystalline fibres and a thin layer of steel/metal on the upper surface of the base.

Conclusions

The developed methodology of solving dynamic contact problems in an elastic-plastic dynamic mathematical formulation makes it possible to model the processes of impact, shock and non-stationary contact interaction with the elastic composite base adequately. In this work, the process of impact on a one-layer glass base reinforced by two rows of fourteen crystalline basalt fibres is adequately modelled and investigated. The fields of summary plastic deformations and normal stresses arising in the base are calculated. The rows of fourteen basalt fibres inside the glass layer redistribute the stresses and plastic deformations that occur in the composite such base. Normal stresses are concentrated in the areas of crystalline basalt fibres. The results obtained make it possible to design new composite reinforced armed materials.

References

1. Bogdanov, V. (2023). *Problems of impact and non-stationary interaction in elastic-plastic formulations*. Cambridge Scholars Publishing. 282. Retrieved from https://www.cambridgescholars.com/product/978-1-5275-9339-8
2. Bogdanov, V. R. (2022). Problem of plane strain state of two-layer body in dynamic elastic-plastic formulation (Part I). *Underwater Technologies*, 12, 3-14. DOI: https://doi.org/10.32347/uwt.2022.12.1101
3. Bogdanov, V. R. (2022). Problem of plane strain state of two-layer body in dynamic elastic-plastic formulation (Part II). *Underwater Technologies*, 12, 15-23. DOI: https://doi.org/10.32347/uwt.2022.12.1102
4. Bogdanov, V. R. (2022). Problem of plane strain state of two-layer body in dynamic elastic-plastic formulation (Part III). International scientific journal "*Transfer of Innovative Technologies*", 5(1), 62-70. DOI: https://doi.org/10.32347/tit.2022.51.0302
5. Bogdanov, V. R. (2022). Problem of plane stress state of two-layer body in dynamic elastic-plastic formulation. *Transfer of Innovative Technologies*, 5, 71-79. DOI :https://doi.org/10.32347/tit.2022.51.0303
6. Lokteva, N. A., Serduk, D. O., Skopintsev, P. D. & Fedotenkov, G. J. (2020) Non-stationary stress-deformed state of a composite cylindrical shell. *Mechanics of Composite Materials and Structures, 26*(4), 544-559, DOI: 10.33113/mkmk, ras.2020.26.04.544_559.08 (in Russian). Retrieved from https://bulletin.incas.ro/files/fedotenkov_makarevskii__all__vol_13_special_issue.pdf
7. Igumnov, L. A., Okonechnikov, A. S., Tarlakovskii, D. V. & Fedotenkov, G. J. (2013). Plane nonsteady-state problem of motion of the surface load on an elastic half-space. *Mathematical Methods and Physicomechanical Fields*, Lviv, 56, 2, 157-163. (in Russian). Retrieved from http://tit.knuba.edu.ua/article/view/275917
8. Kuznetsova, E. L., Tarlakovsky, D. V., Fedotenkov, G. J. & Medvedsky, A. L. (2013). Influence of non-stationary distributed load on the surface of the elastic layer, Works MAI. 71, 1-21 (in Russian). Retrieved from http://tit.knuba.edu.ua/article/view/275917
9. Fedotenkov, G. J., Tarlakovsky, D. V. & Vahterova, Y. A. (2019). Identification of Non-stationary Load Upon Timoshenko Beam, Lobachevskii. *Journal of Mathematics, 40*(4), 439-447. Retrieved from http://tit.knuba.edu.ua/article/view/275917
10. Vahterova, Y. A. & Fedotenkov, G. J. (2020). The inverse problem of recovering an unsteady linear load for an elastic rod of finite length. *Journal of Applied Engineering Science, 18*(4), 687-692, DOI: 10.5937/jaes0-28073. Retrieved from http://tit.knuba.edu.ua/article/view/275917
11. Gorshkov, A. G. & Tarlakovsky, D.V. (1985). Dynamic contact problems with moving boundaries. *Nauka, Fizmatlit*, 352 (in Russian). Retrieved from http://tit.knuba.edu.ua/article/view/275917
12. Bogdanov, V. R. (2018). Impact a circular cylinder with a flat on an elastic layer. *Transfer of In-novative Technologies, 1*(2), 68-74, DOI: 10.31493/tit1812.0302. Retrieved from http://tit.knuba.edu.ua/article/view/275917
13. Mahnenko, V. I. (1976). Computational methods for studying the kinetics of welding stresses and deformations. *Naukova Dumka*, Kiev, 320 (in Russian). Retrieved from http://tit.knuba.edu.ua/article/view/275917
14. Mahnenko, V. I. (2003). Improving methods for estimating the residual life of welded joints in long-life structures. *Automatic welding*, Kiev, 10–11, 112–121 (in Russian). Retrieved from http://tit.knuba.edu.ua/article/view/275917
15. Mahnenko, V. I., Pozniakov, V. D., Velikoivanenko, E. A., Rozynka, G. F. & Pivtorak, N. I. (2009). Risk of cold cracking when welding structural high-strength steels, Collection of scientific works "*Pro-cessing of materials in mechanical engineering*", National Shipbuilding University, 3, 5–12 (in Rus-sian). Retrieved from http://tit.knuba.edu.ua/article/view/275917
16. Kachanov, L. M. (1969). *Fundamentals of the theory of plasticity*. Nauka, Moscow, 420 (in Rus-sian). Retrieved from http://tit.knuba.edu.ua/article/view/275917
17. 1948. *Collection: Theory of plasticity IL*, Moscow, 460. (in Russian). Retrieved from http://tit.knuba.edu.ua/article/view/275917
18. Boli, B., &Waner, G. (1964). *Theory of thermal stresses, Mir, Moscow*, 360 (in Russian). Retrieved from http://tit.knuba.edu.ua/article/view/275916
19. Hemming, R. V. (1972). *Numerical methods, Nauka, Moscow*, 399 (in Russian). Retrieved from http://tit.knuba.edu.ua/article/view/275916
20. Zukina, E. L. (2004). Conservative difference schemes on non-uniform grids for a two-dimensional wave equation. Work of N.I. Lobachevski Math. Centre, Kazan, .26, 151–160 (in Rus-sian). Retrieved from http://tit.knuba.edu.ua/article/view/275916
21. Weisbrod, G. & Rittel, D. (2000). A method for dynamic fracture toughness determination using short beams. *International Journal of Fracture*, 104, 89–103. Retrieved from http://tit.knuba.edu.ua/article/view/275916.